Experimental evidence for a two-band superconducting state of $NbSe_2$ single crystals

M. Zehetmayer[1] and H. W. Weber[1]

[1] *Vienna University of Technology, Atominstitut, 1020 Vienna, Austria**

We report on measurements and a detailed analysis of the reversible magnetization of superconducting $NbSe_2$ single crystals. By comparing the experimental data with Ginzburg Landau theory we show that superconductivity in $NbSe_2$ cannot be explained by an anisotropic single-band, but by a multi-band scenario. Applying a simple two-band model reveals the basic mixed-state parameters, which are quite different in the two bands. We identify a strongly anisotropic band that determines the properties at high magnetic fields, and a second almost isotropic band that dominates at low fields. Our method is well suited for distinguishing anisotropic single-band from multi-band superconductivity in various materials.

PACS numbers: 74.25.Ha,74.25.Op,74.70.Ad

I. INTRODUCTION

$NbSe_2$ is certainly one of the most intensively studied superconducting materials for several reasons. First, its transition temperature (T_c) is about 7 K and its upper critical field not much larger than 4 T perpendicular (B_{c2}^{c}, c-direction) and 12 T parallel (B_{c2}^{ab}, ab-direction) to the Nb planes.[1] Accordingly, most part of the superconducting phase diagram is accessible to experiment, in contrast to many other materials. Furthermore, large high quality single crystals with almost negligible vortex pinning effects can be grown. Introducing a small amount of disorder (e.g. by particle irradiation) may lead to the emergence of the well known fishtail effect,[2] which is still discussed a lot by the superconductivity community. Moreover, $NbSe_2$ was the first material, in which scanning tunneling microscopy was successfully employed for observing vortex cores or distributions[3,4] and it is still widely used for such investigations. Finally, the charge density wave state, formed below about 33 K,[5] allows studying the effect of competing order parameters, which is an important issue for high temperature superconductors.

Recently, $NbSe_2$ was suggested to be a two- or multi-band superconductor, which was confirmed by several experiments (e.g. Refs. 6–11), but usually an alternative interpretation of the results in terms of an anisotropic s-wave single-band scenario could not be excluded. In this paper we provide further evidence for the two-band scenario. The field dependence of the reversible magnetization - $M(B)$ - is compared with Ginzburg Landau theory, showing that $M(B)$ cannot be reliably described by the anisotropic single-band scenario, but by multi-band superconductivity. Evaluating the curves reveals the anisotropy and other superconducting parameters which are not only temperature but also significantly field dependent.

More generally, following the discovery of superconductivity in MgB_2, multi-band scenarios were announced for a lot of materials including Fe-pnictides, borocarbides, heavy fermions, and even cuprates,[12–16] etc. However, the experimental evidence was often based on poor arguments (like, e.g., the observation of a temperature dependent anisotropy) and the anisotropic single-band scenario could rarely be eliminated. Therefore, a method for distinguishing between the two scenarios is clearly desirable, which is provided by our approach. At the same time, all basic mixed state parameters can be assessed in this way.

II. EXPERIMENT AND EVALUATION

Two $NbSe_2$ single crystals grown by a standard chemical vapor transport technique with sizes $a \times b \times c \simeq 2.25 \times 2 \times 0.1$ mm^3 and $1 \times 1 \times 0.1$ mm^3 were investigated. Both have a T_c of 7.15 K and a small transition width of about 0.1 K. The smaller crystal was mainly used for confirming the results of the larger one.

Measurements of the magnetic moment parallel to the applied field (m) as a function of the applied field ($\mu_0 H_a \leq 7$ T, $\mu_0 = 4\pi \times 10^{-7}$ T m A^{-1}) were carried out at temperatures from 2 K to about 10 K in our SQUIDs. The curve above T_c (at 10 K) was subtracted from the superconducting signal to get rid of the temperature independent background signal (which was non-significant in most cases). In all measurements, most parts of the magnetization curves were reversible. Therefore, the reversible magnetization could be obtained directly from $M = m/V$ (V is the sample volume). In the case of irreversibility, the reversible signal had to be calculated from the irreversible parts at increasing (m_+) and decreasing (m_-) field via $M = (m_+ + m_-)/2V$. Minor corrections to the field coming from the critical current were considered numerically as described in Ref. 17. Finally, the magnetic induction B was evaluated via $B = \mu_0(H_a - DM + M)$, where D is the demagnetization factor of the sample, and $M(B)$ obtained. Fitting $M(B)$ from single-band Ginzburg Landau (GL) theory to the experiment results in two parameters, the upper critical field (B_{c2}), which is the field where $M(B > 0)$ vanishes for the first time, and κ, the GL parameter. For simplicity, the GL results were approximated by simpler (but quite accurate) equations given in Ref. 18 (we used Eq. 23 of that reference leading

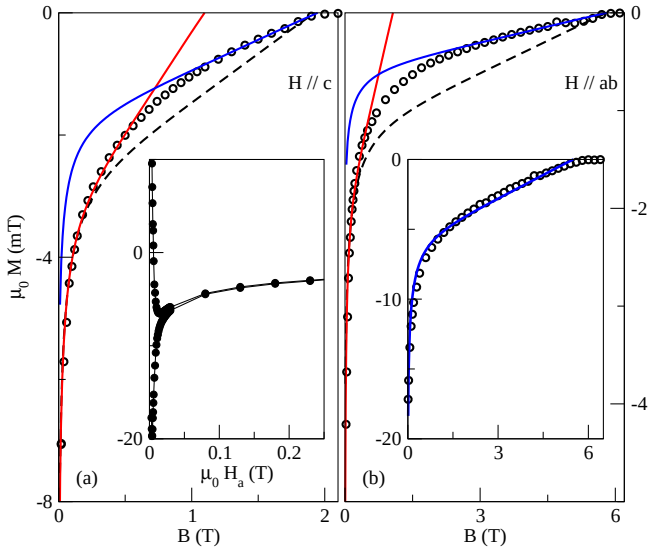

FIG. 1: (Color online) The reversible magnetization from experiment and GL theory. The open circles illustrate the experimental data of $NbSe_2$ for $H_a \parallel c$ (panel a) and $H_a \parallel ab$ (panel b) at 4.2 K. The dashed lines present the best single-band GL fits to the whole field interval, the solid lines to the low- or high-field region only. The inset of panel (a) shows a measured hysteresis loop from which the reversible data has been evaluated. The inset of panel (b) presents the reversible magnetization of a V_3Si single crystal at 13.5 K (open symbols) and the best GL fit (solid line).

to deviations from the exact behavior by less than 3.5%). We point out that other approximations or even numerical solutions of the reversible magnetization $M(B)$ may be applied, which are obtained from GL theory or other models.

III. RESULTS AND DISCUSSION

A. Fitting the reversible magnetization by single- and two-band models

Figure 1 presents results of the experiments and the fitting procedure. The full circles in the inset of panel (a) show the low-field part of the measured magnetization loop m/V for $H_a \parallel c$ at 4.2 K. A significant hysteresis occurs only at very low fields (below about 20 mT, which is $\sim 0.01 B_{c2}$) and this region was excluded from the reversible curves presented by the open circles in the figure. The dashed lines show the best single-band GL fit to the whole superconducting part (from about $0.01 B_{c2}$ to B_{c2}) and therefore represent the results we expect from a single-band superconductor. Here, κ was the only fit parameter while B_{c2} was taken from the point, where the experimental curves reach zero. Enormous differences between experiment and the best GL fits are evident (e.g. Fig. 1) at both field directions and all temperatures (2 - 6.6 K). These deviations become even more apparent when fitting the GL theory only to the high- or low-field region (in the latter case, also B_{c2} is fitted) as illustrated by the solid lines in Fig. 1. We conclude that $NbSe_2$ obviously does not behave like an anisotropic single-band superconductor.

The GL theory holds strictly only sufficiently close to the phase transition and T_c. At low temperatures and far from B_{c2} some deviations are expected, but usually GL theory is quite successful over the whole field and temperature range. Nevertheless, to clarify this point, we fitted the single-band GL theory to magnetization curves of Nb and V_3Si, which are single-band superconductors. In all cases the GL fit showed reliable agreement with experiment over the whole field range, as illustrated, e.g., in the inset of Fig. 1(b) for V_3Si. Fair agreement between GL theory and $M(B)$ data was also found in the more anisotropic superconductors[19–21] $YBa_2Cu_4O_8$, $Nd_{1.85}Ce_{0.15}CuO_{4-\delta}$, and $YBa_2Cu_3O_{7-\delta}$.

In the next step we analyzed possible two-band effects. In the anisotropic single-band scenario, properties like the energy gap or the coupling strength vary within one band, while in the multi-band model[22] superconducting charge carriers exist in two (or more) electron bands at the Fermi surface characterized by two (or more) sets of parameters. Two-band behavior can be observed if two of the parameter sets are significantly different, e.g. for the upper critical field or the anisotropy, and if both bands contribute substantially to the overall properties. Additionally, interband coupling (pairing of electrons from different bands) is expected, which leads, e.g., to one single transition temperature of both bands. Even quite small interband coupling strengths would strongly mask the superconducting transition of the band with the lower values of T_c and B_{c2}, which, however, does not mean that the properties follow the behavior of a conventional single-band superconductor.[23] While the temperature dependence of most quantities is often quite similar for anisotropic single-band and two-band materials, the field dependence is rather different. To analyze two-band effects in the experiment, we separated $M(B)$ into a high- and a low-field region and fitted both regions independently by single-band GL theory (see solid lines of Fig. 1).

In the high-field region, good agreement was achieved in the range from about 0.6 B_{c2}^c to B_{c2}^c for $H_a \parallel c$ and from 0.5 B_{c2}^{ab} to B_{c2}^{ab} for $H_a \parallel ab$ at all temperatures. This indicates that superconductivity of the second band is suppressed at those high-fields and only the single-band properties of the band with the larger upper critical field (indicated by the superscript 'α') survive. Some effects of interband coupling cannot be excluded, but are expected to be small. Accordingly, the high-field GL fit is assumed to roughly provide the single-band parameters of the α-band (see Fig. 2 and Tab. I).

Turning to lower fields in Fig. 1, the discrepancy between the experimental data and the high-field single-band GL fit increases, which we ascribe to the influence of a second band with a smaller B_{c2} (superscript β).

With decreasing field the β-band becomes more dominant (particularly for $H_a \parallel ab$), but the contribution of $M^\alpha(B)$ does not become negligible. Therefore, single-band behavior is not expected and the low-field GL fit only provides effective parameters (index 'lf') of the overall superconducting behavior, although more indicative of the β-band. The fit interval ranged from $0.05B_{c2}^c$ to $0.3B_{c2}^c$ for $H_a \parallel c$, which was the largest interval that enabled good matching at all temperatures. The fit parameters are more affected by reducing the interval than in the high-field regime, but the major findings are not concerned. To be consistent, we applied the same field interval in absolute values for $H_a \parallel ab$, which roughly corresponds to $0.016B_{c2}^{ab}$ to $0.1B_{c2}^{ab}$.

To come closer to the single-band properties of the β-band, we subtracted the α-band GL fit from the experimental data. However, pure single-band behavior of the remaining $M(B)$ ($M^\beta(B)$) is still not expected and indeed not observed due to interband coupling (which might dominate, where $M^\beta(B)$ approaches zero, i.e. near B_{c2} of the β-band) and possible additional superconducting bands. Accordingly, the field interval, where single-band GL theory matched well was similar as for the effective 'lf' regime before subtracting the α-band. In contrast to the 'lf' regime, however, the thermodynamic critical field (B_c, see Tab. I) of the β-band is almost independent of the field orientation as expected for a single band (small deviations are ascribed to the interband coupling and experimental uncertainties).

B. Mixed-state properties and anisotropy

The results of the fitting procedure are illustrated in Fig. 2 and Tab. I. $B_{c2}^{c,\alpha}$ (α-band) follows well the behavior of simple conventional superconductors (full circles in Fig. 2(a)). For extrapolating the data to 0 K the model $B_{c2}(T) = B_{c2}(0)[1-(T/T_c)^a]^b$ (lines in Fig. 2(a)) was applied which matches best for $a \simeq 1.3$, $b \simeq 1$, and $B_{c2}^{c,\alpha}(0\,\mathrm{K}) \simeq 4.1\,\mathrm{T}$. The same model leads to $B_{c2}^{ab,\alpha}(0\,\mathrm{K}) \simeq 12.3\,\mathrm{T}$ ($H_a \parallel ab$). In the latter case, we observe a positive curvature of B_{c2} near T_c, while $B_{c2}^{c,\alpha}$ is linear in this regime. The corresponding GL parameters (κ, Fig. 2(b)) decrease strongly with increasing temperature. Extrapolation gives roughly $\kappa^{c,\alpha}(0\,\mathrm{K}) \simeq 30$ and $\kappa^{c,\alpha}(6\,\mathrm{K}) \simeq 17$ as well as $\kappa^{ab,\alpha}(0\,\mathrm{K}) \simeq 86$ and $\kappa^{ab,\alpha}(6.6\,\mathrm{K}) \simeq 30$.

The β-band upper critical fields are also well fitted by the above model leading to much smaller results at 0 K, namely $B_{c2}^{c,\beta}(0\,\mathrm{K}) \simeq 1.6\,\mathrm{T}$ and $B_{c2}^{ab,\beta}(0\,\mathrm{K}) \simeq 1.9\,\mathrm{T}$. Also the GL parameters decrease and show a less pronounced temperature dependence, i.e., $\kappa^{c,\beta}(0\,\mathrm{K}) \simeq 15$ and $\kappa^{c,\beta}(6\,\mathrm{K}) \simeq 15$, $\kappa^{ab,\beta}(0\,\mathrm{K}) \simeq 21$, $\kappa^{ab,\beta}(6\,\mathrm{K}) \simeq 19$. The effective parameters (which address the sum of the α- and β-band) of the low-field regime deviate only slightly from the β-band data (see Fig. 2 and Tab. I).

The above results lead to the anisotropies $\gamma_{Bc2} = B_{c2}^{ab}/B_{c2}^{c}$ and $\gamma_\kappa = \kappa^{ab}/\kappa^{c}$ illustrated in panel (c) of Fig. 2. At high fields (α-band) and temperatures below $\sim 5\,\mathrm{K}$, $\gamma_{Bc2} \simeq 3$ and almost constant (open circles), i.e. close to the value usually reported for $NbSe_2$,[1] but drops to 2.3 at 7 K. Such a temperature dependence corresponds to the positive curvature of $B_{c2}^{ab}(T)$ near T_c and is, in general, a characteristic of both, two-band[14] and anisotropic single-band[24] superconductivity. The anisotropy of κ (full circles) is almost identical to γ_{Bc2} (open circles) in the high-field regime. At lower fields the anisotropy of the GL properties is considerably reduced. We obtain $\gamma^\beta \simeq 1.3$ ($\gamma_{Bc2} \simeq 1.2$, $\gamma_\kappa \simeq 1.4$) and $\gamma^{lf} \simeq 1.35$ ($\gamma_{Bc2} \simeq 1.2$, $\gamma_\kappa \simeq 1.5$), thus almost isotropic behavior. The small differences in γ_{Bc2} and γ_κ could result from the larger experimental uncertainties in this regime.

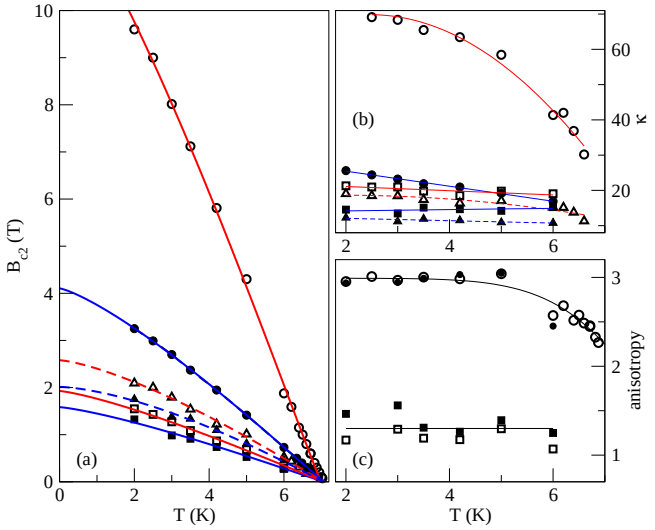

FIG. 2: (Color online) The superconducting parameters of $NbSe_2$ obtained from evaluating the reversible magnetization curves. Panel (a) displays the upper critical fields (B_{c2}), panel (b) the Ginzburg Landau parameters (κ), and panel (c) the anisotropies. The circles (with solid lines) present α-band, the squares (with solid lines) β-band, and the triangles (with dashed lines) effective low-field regime results. In panel (a) and (b) the open symbols refer to $H_a \parallel ab$ and the full symbols to $H_a \parallel c$, in panel (c) to the B_{c2} (open) and the κ (full) anisotropies. The lines are guides for the eyes.

In summary, the anisotropy of $NbSe_2$ changes strongly with the applied field from a large value (~ 3) at high fields ($\gtrsim 0.5B_{c2}$) to almost isotropic behavior at low fields ($\lesssim 0.3B_{c2}^c$, $\lesssim 0.1B_{c2}^{ab}$). It seems impossible to explain this behavior by a single-band model, i.e. a two- or multi-band model is needed. Our results suggest the existence of a strongly anisotropic (α) band with a large B_{c2}, and a second almost isotropic (β) band with a lower B_{c2} (or, to be consistent with two-band theory: both bands may have the same B_{c2} due to interband coupling, but the properties of the β-band are strongly suppressed at high fields). We further point out, that the anisotropies of B_{c2} and κ are equal or quite similar, when acquired at the same field and temperature. Accordingly, this holds also for the anisotropy of all further parameters, such

TABLE I: Summary of mixed-state parameters of single crystalline $NbSe_2$ at 0 K in the α- and β-band and the effective low-field ('lf') regime. Minor inconsistencies with the GL relations occur from extrapolating the experimental data to 0 K.

	α	β	lf		α	β	lf
B_{c2}^{c} (T):	4.1	1.6	2.0	B_{c2}^{ab} (T):	12.3	1.9	2.6
B_{c1}^{c} (mT):	9.0	11.4	19.1	B_{c1}^{ab} (mT):	3.9	7.7	10.3
B_{c}^{c} (mT):	98	67	112	B_{c}^{ab} (mT):	98	64	86
λ_{ab} (nm):	265	215	165	λ_{c} (nm):	795	355	350
ξ_{ab} (nm):	9	14	13	ξ_{c} (nm):	3	12	10
κ^{c}:	30	15	13	κ^{ab}:	86	21	21
γ:	3.0	1.3	1.4				

as the magnetic penetration depth (λ) or the coherence lengths (ξ). These anisotropies were often claimed to be quite different in the two-band superconductor MgB_2. But detailed evaluations showed that the situation is actually the same as in $NbSe_2$, i.e. all parameters have the same anisotropy.[25] The misinterpretation in MgB_2 usually originated from measuring the anisotropies of different properties at different applied fields, e.g. that of ξ at high fields (from the B_{c2} anisotropy) and that of λ at low fields.

Further parameters were calculated by applying the well known GL relations (e.g. Ref. 26), namely ξ, λ, B_c, and B_{c1} (the lower critical fields). The temperature dependence of these quantities was fitted by the same (general) model as B_{c2} and the results at 0 K are listed in Tab. I. Additionally, B_c of the whole sample was obtained from integrating the reversible magnetization curve,[26] i.e. $-\mu_0 \int_0^{Hc2} MdH = B_c^2/(2\mu_0)$, resulting in about 120 mT at 0 K.

C. Discussion

Our results are consistent with most findings from literature. For instance, the Fermi level of $NbSe_2$ is known to be crossed by three electron bands, one is related to Se-4p orbitals and shows a rather three dimensional pancake like sheet, and the other two to Nb-4d orbitals each leading to two rather two-dimensional (cylindrical) Fermi sheets.[27] There is general consensus that a superconducting gap opens in both Nb bands. Investigations by ARPES[6] at 5.3 K resulted in gap values of 0.9 - 1.0 meV, but no gap was detected on the Se bands. On the other hand, scanning tunneling spectroscopy[8,28] revealed a broader range of gap values from about 1.4 to 0.7 (or even 0.4) meV close to 0 K. The band, on which the smaller gaps exist, was not clearly identified, but it was argued, that the smaller gaps may open on the Se bands, which would not necessarily contradict the ARPES measurements, since the smaller gap could be suppressed near T_c in a two-band model.[8] It is plausible to associate the α-band, which has the higher B_{c2}, with the larger gap (Δ_α) and thus the β-band with the smaller gap (Δ_β). The fact that the superconducting properties of the β-band are nearly isotropic may favor assigning Δ_β to the more three dimensional Se-band. On the other hand, ab-initio calculations revealed that the electron density of states of the Se band at the Fermi level - $z(0)$ - is only about 5 % of the overall value,[27] which makes a substantial contribution of the Se bands to the superconducting behavior questionable. Moreover, applying the BCS relations for the condensation energy density $E_c = -z(0)\Delta^2/2 = -B_c^2/(2\mu_0)$ with B_c from Tab. I, results in similar $z(0)$ values for both bands, as was actually found for the two Nb bands in Ref. 27 and thus favors a scenario, in which the two Nb bands are responsible for the two-band effects. It may be concluded that some microscopic aspects remain unclear and need further investigations. We note further that our results are in fair agreement with those from a specific-heat study.[10] Fitting the field dependence of the specific heat data by a simple two-band model led to similar upper critical fields and anisotropies of the two bands as in our study.

Finally, we wish to mention the remarkable qualitative resemblance of the two-band properties in $NbSe_2$ and MgB_2, for which a similar analysis[25] also demonstrated a highly anisotropic band (σ-band) being dominant at high magnetic fields and a quite isotropic low-field band (π-band), with similar values for the upper critical fields and the anisotropies, but a larger transition temperature (of almost 40 K). We point out that the mixed-state parameters obtained by our approach in MgB_2 are in good agreement with results derived from other methods, even for the band with the lower B_{c2}.

There is also cumulative evidence for multi-band superconductivity in the family of the Fe-pnictide superconductors (e.g. Refs. 12,13). Contrary to $NbSe_2$ and MgB_2, however, the anisotropy of the upper critical field (i.e., the high-field value of γ) seems to be smaller than that at low fields[29,30](i.e. the anisotropy of the penetration depth or of the lower critical field). This would indicate that the band with the larger upper critical field is less anisotropic. More recent results suggest, however, that a proper description of experimental data is only possible by taking three or more bands into account.[31,32] Further insight might be gained when reversible magnetization curves over the whole field range become available for these materials.

IV. SUMMARY

In summary, we have shown that the reversible magnetization of $NbSe_2$ cannot be reliably explained by a standard anisotropic single-band scenario. Applying a simple two-band model reveals the anisotropy and other mixed-state parameters as a function of magnetic field and temperature. We found a strongly anisotropic band ($\gamma \simeq 3$) that dominates at high fields and a second almost isotropic band relevant only at low fields. The method can be applied to other materials to distinguish between

single-band and multi-band superconductivity and to acquire at the same time all basic mixed-state parameters.

Acknowledgments

The authors thank P. H. Kes for providing samples and A. Kremsner and C. Trauner for carrying out some of the measurements. This work was supported by the Austrian Science Fund under contract 21194.

* Electronic address: zehetm@ati.ac.at

[1] D. Sanchez, A. Junod, J. Muller, H. Berger, and F. Levy, Physica B **204**, 167 (1995).
[2] S. Bhattacharya and M. J. Higgins, Phys. Rev. Lett. **70**, 2617 (1993).
[3] H. F. Hess, R. B. Robinson, R. C. Dynes, J. M. Valles, and J. V. Waszczak, Phys. Rev. Lett. **62**, 214 (1989).
[4] H. F. Hess, R. B. Robinson, and J. V. Waszczak, Phys. Rev. Lett. **64**, 2711 (1990).
[5] D. E. Moncton, J. D. Axe, and F. J. DiSalvo, Phys. Rev. Lett. **34**, 734 (1975).
[6] T. Yokoya, T. Kiss, A. Chainani, S. Shin, M. Nohara, and H. Takagi, Science **294**, 2518 (2001).
[7] E. Boaknin, M. A. Tanatar, J. Paglione, D. Hawthorn, F. Ronning, R. W. Hill, M. Sutherland, L. Taillefer, J. Sonier, S. M. Hayden, et al., Phys. Rev. Lett. **90**, 117003 (2003).
[8] J. G. Rodrigo and S. Vieira, Physica C **404**, 306 (2004).
[9] J. D. Fletcher, A. Carrington, P. Diener, P. Rodière, J. P. Brison, R. Prozorov, T. Olheiser, and R. W. Giannetta, Phys. Rev. Lett. **98**, 057003 (2007).
[10] C. L. Huang, J.-Y. Lin, Y. T. Chang, C. P. Sun, H. Y. Shen, C. C. Chou, H. Berger, T. K. Lee, and H. D. Yang, Phys. Rev. B **76**, 212504 (2007).
[11] M. D. Hossain, Z. Salman, D. Wang, K. H. Chow, S. Kreitzman, T. A. Keeler, C. D. P. Levy, W. A. MacFarlane, R. I. Miller, G. D. Morris, et al., Phys. Rev. B **79**, 144518 (2009).
[12] F. Hunte, J. Jaroszynski, A. Gurevich, D. C. Larbalestier, R. Jin, A. S. Sefat, M. A. McGuire, B. C. Sales, D. K. Christen, and D. Mandrus, Nature **453**, 903 (2008).
[13] I. I. Mazin, D. J. Singh, M. D. Johannes, and M. H. Du, Phys. Rev. Lett. **101**, 057003 (2008).
[14] S. V. Shulga, S.-L. Drechsler, G. Fuchs, K.-H. Müller, K. Winzer, M. Heinecke, and K. Krug, Phys. Rev. Lett. **80**, 1730 (1998).
[15] G. Seyfarth, J. P. Brison, M.-A. Méasson, J. Flouquet, K. Izawa, Y. Matsuda, H. Sugawara, and H. Sato, Phys. Rev. Lett. **95**, 107004 (2005).
[16] R. Khasanov, S. Strässle, D. Di Castro, T. Masui, S. Miyasaka, S. Tajima, A. Bussmann-Holder, and H. Keller, Phys. Rev. Lett. **99**, 237601 (2007).
[17] M. Zehetmayer, Phys. Rev. B **80**, 104512 (2009).
[18] E. H. Brandt, Phys. Rev. B **68**, 054506 (2003).
[19] W. V. Pogosov, K. I. Kugel, A. L. Rakhmanov, and E. H. Brandt, Phys. Rev. B **64**, 064517 (2001).
[20] A. Achalere and B. Dey, Phys. Rev. B **71**, 224504 (2005).
[21] M. Karmakar and B. Dey, Phys. Rev. B **74**, 172508 (2006).
[22] H. Suhl, B. T. Matthias, and L. R. Walker, Phys. Rev. Lett. **3**, 552 (1959).
[23] E. J. Nicol and J. P. Carbotte, Phys. Rev. B **71**, 054501 (2005).
[24] W. Pitscheneder and E. Schachinger, Phys. Rev. B **47**, 3300 (1993).
[25] M. Zehetmayer, M. Eisterer, J. Jun, S. M. Kazakov, J. Karpinski, and H. W. Weber, Phys. Rev. B **70**, 214516 (2004).
[26] M. Tinkham, *Introduction to superconductivity* (McGraw-Hill, New York, 1975).
[27] M. D. Johannes, I. I. Mazin, and C. A. Howells, Phys. Rev. B **73**, 205102 (2006).
[28] I. Guillamon, H. Suderow, F. Guinea, and S. Vieira, Phys. Rev. B **77**, 134505 (2008).
[29] R. Khasanov, D. V. Evtushinsky, A. Amato, H.-H. Klauss, H. Luetkens, C. Niedermayer, B. Büchner, G. L. Sun, C. T. Lin, J. T. Park, et al., Phys. Rev. Lett. **102**, 187005 (2009).
[30] S. Weyeneth, R. Puzniak, N. D. Zhigadlo, S. Katrych, Z. Bukowski, J. Karpinski, H. Keller, J. Supercond. Novel Magnetism **22**, 347 (2009).
[31] G. A. Ummarino, M. Tortello, D. Daghero, and R. S. Gonnelli, Phys. Rev. B **80**, 172503 (2009).
[32] K. W. Kim, M. Rössle, A. Dubroka, V. K. Malik, T. Wolf, and C. Bernhard, Phys. Rev. B **81**, 214508 (2010).